Journal of Materials Chemistry

Dynamic Article Links

Cite this: *J. Mater. Chem.*, 2011, **21**, 16686

www.rsc.org/materials

FEATURE ARTICLE

Self-assembly and flux closure studies of magnetic nanoparticle rings†

Alexander Wei,*[ab] Takeshi Kasama[c] and Rafal E. Dunin-Borkowski[c]

Received 2nd May 2011, Accepted 9th August 2011
DOI: 10.1039/c1jm11916h

Thermoremanent magnetic nanoparticles (MNPs) can self-assemble into rings through dipolar interactions, when dispersed under appropriate conditions. Analysis of individual MNP rings and clusters by off-axis electron holography reveals bistable flux closure (FC) states at ambient temperatures, and their reversible switching by magnetic field gradients. We introduce a line-bond formalism to describe the coupling between MNPs.

Introduction

Magnetic nanostructures with well-defined remanent states are appealing candidates as memory cells and switches for nonvolatile random-access memory (NVRAM) devices.[1,2] Annular nanomagnets are of particular interest for their capacity to support bistable magnetic states known as flux closure (FC; Fig. 1).[3,4] These vortex-like domains can be polarized either clockwise (CW) or counterclockwise (CCW) but maintain a net magnetostatic energy of zero, with minimum stray flux inside and outside the ring. The latter feature allows FC states to coexist in close proximity with minimal coupling, and support architectures for high-density data storage.

The polarization of FC states can be switched by a magnetic field gradient, most notably that produced by an electrical current passing through the ring's center. FC switching of millimetre-sized ferrite rings provided the basis for core memories in earlier computer technologies, prior to the advent of semiconductor-based devices.[5,6] More recently, FC states are being considered for NVRAM and related magnetoelectronic applications, based on nanosized bits.[1,2] The fundamental limit in the FC switching rate has been determined to be in the low picosecond range, orders of magnitude faster than switching speeds in present-day microprocessors.[7]

The size threshold for stable FC states in magnetic rings is defined by the single-domain limit, and in turn by the magnetocrystalline anisotropy of the host material.[8] For magnetic materials such as Co and $Fe_{20}Ni_{80}$ (Permalloy), this threshold is in the tens of nanometres, but top-down methods such as electron-beam lithography cannot reproducibly fabricate annular structures much below 100 nm.[9] However, single-domain magnetic nanoparticles (MNPs) are readily accessible by chemical synthesis, and can be used to create nanostructures much smaller than those produced by top-down lithography. In particular, MNPs with magnetic remanence at room temperature (*i.e.*, a nonzero moment at zero field) are capable of dipole-directed self-assembly into higher-order structures. Dipolar potentials scale as a function of μ^2/D^3, where μ is the MNP moment and D is the distance between particle centers. Directional self-assembly becomes possible when the potential is significantly above thermal energy levels, or several times kT.

The dipolar assembly of thermoremanent MNPs into chains is well known,[10,11] but their controlled self-assembly into rings was mostly hypothetical until ten years ago.[12,13] Reproducible conditions for the dipole-directed assembly of MNP rings were first described by Wei and coworkers,[14,15] and several more examples have been reported since then.[16–19] Part of the challenge has been to identify specific conditions for ring assembly, which involve a fine balance between enthalpic dipolar interactions and entropic factors in solution stabilization. The deposition of rings onto surfaces must also be carefully controlled to minimize the influence of dissipative forces on the final self-assembled structures.

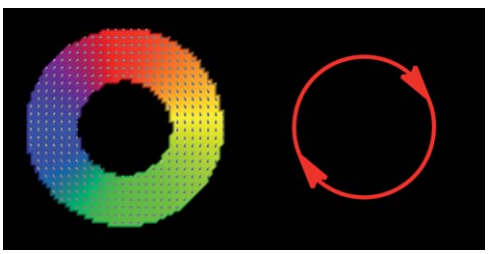

Fig. 1 Micromagnetics simulation of flux closure (FC) in a magnetic ring, with CW polarization. The phase of local magnetic induction can be mapped according to a color wheel (*left*), whereas the FC polarization can be simply described by circulating arrows (*right*).

[a]*Department of Chemistry, Purdue University, 560 Oval Dr., West Lafayette, IN, 47907, USA. E-mail: alexwei@purdue.edu; Fax: +1-765-494-0239; Tel: +1-765-494-5257*

[b]*Birck Nanotechnology Center, Purdue University, West Lafayette, IN, USA*

[c]*Center for Electron Nanoscopy, Technical University of Denmark, DK-2800 Kongens, Lyngby, Denmark*

† This work was supported in part by grants from the National Science Foundation (CHE-0243496, CHE-0957738) and the Defense Advanced Research Project Agency. We also gratefully acknowledge Steven Tripp, Jie Liu, and Michael Scheinfein for their many experimental and theoretical contributions to this work.

In this article we present experimental and analytical studies on the self-assembly of thermoremanent Co nanoparticles into MNP rings with collective FC states. Many of these rings are less than 100 nm across, yet are able to support bistable FC states at room temperature (Fig. 2).[15,20] These FC states can be imaged with nanometre resolution by off-axis electron holography (EH), a specialized TEM technique that measures the in-plane magnetic induction produced by MNPs and their assemblies at zero field.[21] The magnetic induction measurements can be mapped in accordance with a color wheel, whereas the polarization of FC states can be described simply by curved-arrow notation. We use EH to show that the FC polarizations of our MNP rings are stable at room temperature, but can be switched by exposure to out-of-plane magnetic pulses.[22] EH analysis also reveals the net direction of each MNP moment, and the coupling between MNPs. We introduce a line-bond formalism to represent the nearest-neighbor couplings within a MNP network, analogous to that used to describe covalent bonding in molecules (Fig. 2, *top*).

Self-assembly of magnetic nanoparticle rings

Thermoremanent Co NPs ($d = 27 \pm 4$ nm) were synthesized by the solvothermal decomposition of $Co_2(CO)_8$, then redispersed in toluene using calixarene **1** as a stabilizing surfactant (Fig. 3).[15] Calixarenes have concave, macrocyclic headgroups that are appended to several hydrocarbon tails, and are outstanding surfactants for dispersing nanoparticles in organic solvents.[14,23] Co NPs ($\sim 10^{13}$ NPs mL^{-1}) stabilized by **1** (10^{6} to 10^{3} M) were deposited and dried on carbon-coated TEM grids in the absence of external magnetic fields, to produce significant populations of bracelet-like NP rings. It should be noted that the Co NPs were encapsulated in thin but stable CoO shells (see below), formed upon initial exposure to air but which preserved the metallic Co cores from further oxidation. This has enabled Co NP suspensions to retain their ability to self-assemble into rings, several years after synthesis.

Several factors contribute toward the favorable formation of MNP rings. First, magnetic dipoles are clearly responsible for the observed ring assemblies at zero field. Smaller, superparamagnetic Co@CoO core–shell NPs ($d < 15$ nm) do not participate directly in dipole-directed self-assembly, and are mostly incorporated as satellites along the perimeters of the MNP rings.[14,15] Second, MNP rings have a lower magnetostatic energy per particle relative to similarly sized chains and clusters, so their self-assembly in solution is thermodynamically favored. Molecular dynamics simulations on discrete ensembles of dipolar particles ($N < 10$) have indicated a marked preference for forming rings rather than chains at zero field.[13] However, ring self-assembly can be disrupted by an applied magnetic field, as the dipoles of individual MNPs will attempt to align with the external field lines and destabilize the collective FC state. This was demonstrated by applying an in-plane magnetic field during sample deposition, resulting in partial transition to oriented MNP chains (Fig. 4a). On the other hand, MNPs previously exposed to magnetic fields could still form rings after sufficient time for relaxation (Fig. 4b), confirming that the dipolar self-assembly of MNP rings is indeed thermodynamically favored over that of chains.[15]

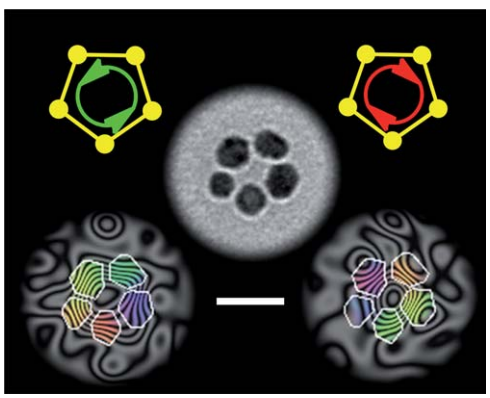

Fig. 2 Self-assembled MNP rings imaged under bright-field TEM conditions (*center*) and by off-axis electron holography (*bottom*). The latter reveals bistable FC states, polarized CCW (*left*) or CW (*right*). Scale bar = 50 nm.

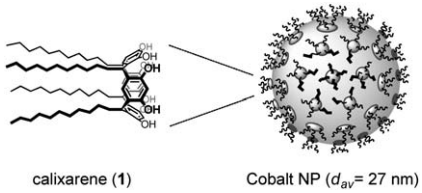

Fig. 3 Thermoremanent cobalt NPs stabilized by calixarene **1**, for their self-assembly into bracelet-like MNP rings.[15] Reprinted with permission from the American Chemical Society.

A third factor in MNP ring self-assembly is the aggregate size distribution in solution, which can be adjusted by manipulating NP concentrations and dispersion conditions. This affects the balance between enthalpic interactions (magnetic dipoles and long-range van der Waals) and statistical entropy. For example, diluting the dispersion of calixarene-stabilized Co@CoO NPs reduced the median ring size, and increased the number of 5- and 6-membered MNP rings with diameters below 100 nm (Fig. 4c).[20] Roughly 20% of all MNPs could be assembled and deposited as rings under these conditions; most of the remaining particles were assembled as short chains or close-packed clusters.

Surfactants also promote the kinetic stability of MNP rings by reducing their collapse into close-packed clusters, either in solution or during substrate deposition. The influence of entropic steric repulsion on self-assembly is subtle, with insights based

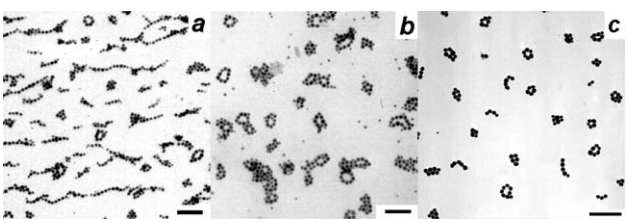

Fig. 4 (a) Self-assembly of MNPs into rings and chains, deposited under the influence of a magnetic field (10^{13} NPs mL^{-1}; $B = 225$ G).[15] (b) MNPs deposited with restoration of ring self-assembly, after removal of magnetic field. Reprinted with permission from the American Chemical Society. (c) Self-assembly of MNPs using a more dilute dispersion (10^{12} NPs mL^{-1}).[20] Scale bar = 200 nm.

largely on empirical evidence. In our studies, MNP rings are not observed when calixarene **1** is replaced with an equal amount of oleic acid, a surfactant commonly used in NP synthesis.[24] Other studies of MNP rings are based on NPs collected from bacterial lysates (with proteins)[16] or solutions containing polymers,[17–19] both of which can contribute to steric stabilization. It is worth noting that the latter condition can produce high yields of MNP rings, possibly stabilized by polymer crosslinking (Fig. 5).[18]

Lastly, sample preparation is an important variable in the characterization of the final MNP assemblies, particularly if electron microscopy is involved. Poor control over dissipative forces during sample deposition and drying can promote the collapse of MNP rings into close-packed clusters or aggregates. Rapid solvent evaporation and substrate dewetting can also produce thermal gradients or instabilities in the residual wetting layer that drive the kinetic deposition of solutes into ring-like mesostructures.[25] Examples of such nonequilibrium processes include hole nucleation,[26] cell wall formation by Rayleigh–Bénard convection,[27] "breath figures" created by water condensation on rapidly cooling surfaces,[28] and contact line pinning during surface dewetting.[29] However, these annular deposits are 1–2 orders of magnitude larger than the bracelet-like nanorings formed by dipolar self-assembly.

The disruptive impact of dissipative forces on MNP ring assembly can be minimized by increasing the viscosity of the wetting layer, and by reducing the evaporation rate after sample deposition. The former effectively fixes the fragile self-assembled structures at an early stage of the drying process, and the latter preserves the dipolar coupling between MNPs. For example, Co@CoO NPs dispersed in CH_2Cl_2 were deposited as radially symmetric mesoscale rings by hole nucleation (Fig. 6a).[15] However, a close inspection of such rings reveals numerous gaps between NPs. In comparison, the spacings of MNP rings cast from toluene solutions are consistently close-packed (Fig. 6b). The absence of gaps in MNP rings formed by dipolar self-assembly ensures maximum interparticle coupling for the collective FC state.

TEM and electron holography analyses

MNP rings formed by dipole-directed self-assembly were deposited onto Cu grids supported by holey carbon films, and initially examined by energy-filtered TEM (also known as electron energy-loss spectroscopy), a chemical imaging technique with nanometre resolution.[30] The elemental distribution maps indicate each MNP to have a core of pure Co, a 3–4 nm shell of

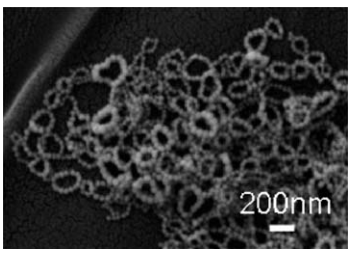

Fig. 5 SEM image of MNP rings formed during the synthesis of Ni_7Co_3 NPs in the presence of poly(vinylpyrrolidone).[18] Reprinted with permission from the American Chemical Society.

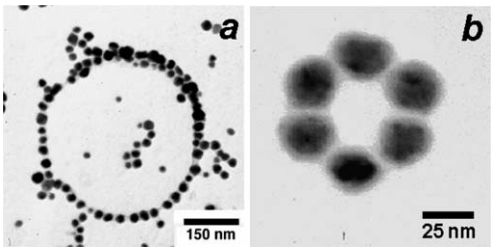

Fig. 6 (a) Mesoscopic ring formed under dissipative conditions, by deposition of MNPs from a CH_2Cl_2 dispersion containing **1**.[15] (b) MNP ring by dipolar self-assembly, deposited from a toluene dispersion. Reprinted with permission from the American Chemical Society.

CoO, and a supporting layer of organic surfactant (Fig. 7b–d).[20,31] The in-plane magnetization of the MNP rings was characterized at 298 K by off-axis EH, which revealed a continuous loop of magnetic induction with a net CW polarization (Fig. 7e and f). The spacing between flux contours is inversely proportional to the flux density, which is greatest within the MNP domains. Minimum stray flux is observed inside the ring, in accord with the magnetostatic description of a FC state.[12]

EH analysis of additional MNP rings reveals each one to have a FC state with either CW or CCW polarization, despite

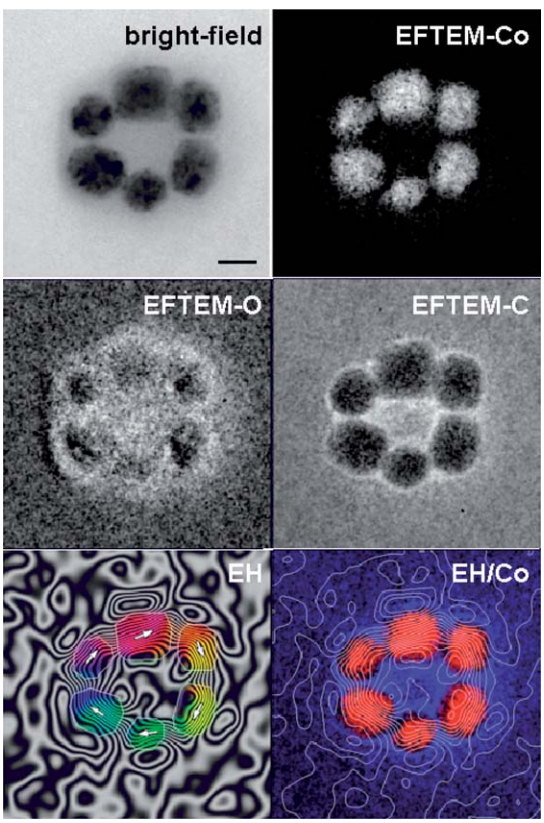

Fig. 7 Energy-filtered TEM and EH analysis of a 6-membered MNP at 298 K. Starting from upper left: bright-field zero-loss image (scale bar = 20 nm); Co elemental map; O elemental map; C elemental map; EH phase contour map of FC state with CW polarization, as indicated by white arrows; EH contour lines (white) superimposed on the Co elemental map. Magnetic flux enclosed between adjacent contours is 0.032 rads ($h/128e$). Reprinted with permission from Taylor and Francis.

variations in size and overall structure (Fig. 8a–f).[31] A racemic distribution of CW and CCW states is assumed, given the absence of a polarization bias. The magnetic flux loop is continuous despite structural defects in the MNPs, or deviations from radial symmetry in the self-assembled rings. We note that "exocyclic" MNPs can also participate in collective FC states, but their presence can cause a divergence in magnetic flux, extending it beyond the outer perimeter of the ring (*e.g.*, Fig. 8f).

FC states can also be found in close-packed MNP clusters (Fig. 8g–l), some supported by as few as three particles. However, the magnetic induction is less tightly confined within these clusters: the divergence of flux from one or more MNPs indicates that their magnetic moments do not contribute fully to the collective FC state. MNP clusters with a central particle (Fig. 8m–o) also form FC states, as opposed to their alignment into a single, ferromagnetic domain. The peripheral MNPs exhibit strongly cooperative dipolar coupling, but the central particle redirects some of the flux across the ring to form smaller FC states. Only chain-like aggregates (Fig. 8q) do not experience FC, but instead favor a single-domain state. Overall, we find that FC states appear whenever MNPs can form a closed loop.

The local magnetic induction and FC states can also be represented by a graphic formalism based on line-bond structures (Fig. 9). This formalism consists of three simple rules. First, nanoparticle "bonds" are drawn between two centroids to represent the flux lines shared between MNPs; arrows serve to indicate the direction of dipolar coupling. Second, unsatisfied dipoles in MNPs can be portrayed as "unoccupied orbitals" for cases where flux divergence is observed. Third, rings can be distinguished from close-packed clusters by introducing a circle within a FC circuit.

While the line-bond formalism has obvious analogies to chemical bonding, these structures are mostly intended to convey the network of dipolar couplings within MNP clusters using common motifs; concepts such as orbital hybridization or conjugation are not considered here. The line-bond formalism also does not address local flux changes within individual MNPs caused by domain walls or twinning defects. Rather, it is a convenient method for describing FC domains in MNP rings and clusters, as well as changes in FC polarization induced by magnetic switching fields.

Flux closure reversal by out-of-plane magnetic fields

The FC states in MNP rings are stable at room temperature, supporting their possible development into memory elements for high-density data storage. As mentioned earlier, the polarization of binary FC states can be switched by external magnetic fields with application toward NVRAM. The FC switching in mesoscale magnetic rings can be driven by applying an in-plane magnetic field ($H_{x,y}$),[32] and current-induced FC reversals (*via* circularly polarized magnetic fields) have been achieved in submicron magnetic cylinders.[33]

For the case of self-assembled MNP rings, EH analysis reveals that their FC polarizations are also reversibly switched by magnetic fields. Remarkably, these FC states can be switched by coaxial magnetic fields (H_z), perpendicular to the plane of the rings.[22] H_z-induced FC switching has not been reported for either macroscopic or mesoscopic magnetic rings, and is possibly exclusive to MNP rings.

In a typical study using EH, MNP rings are initially subjected to a strong coaxial magnetic field ($H_z = +2$ T). This is simply a consequence of electron-beam focusing during routine TEM

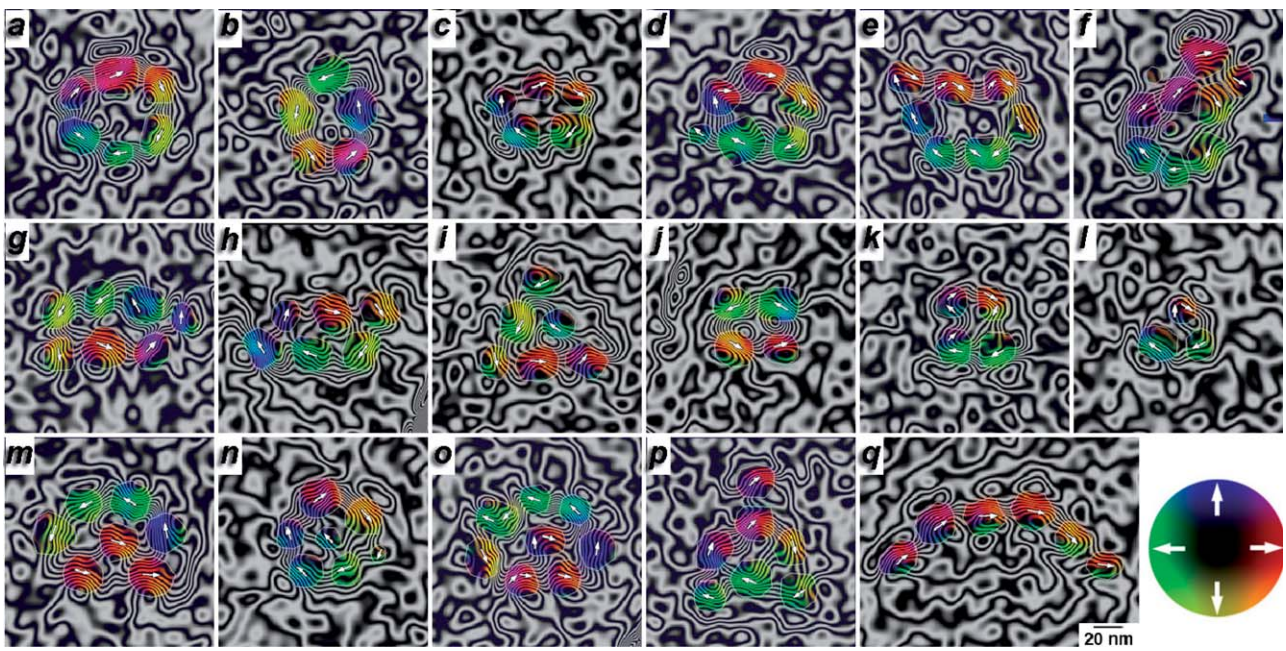

Fig. 8 EH phase contour maps of MNP rings and clusters. (a–e) MNP rings; (f) ring with peripheral (exocyclic) MNPs; (g–l) close-packed MNP clusters; (m–o) MNP clusters with internal particle; (p) cluster with peripheral particle; and (q) MNP chain. The phase of magnetic induction is encoded according to a color wheel (legend at lower right); the net magnetizations of local domains are indicated by white arrows. Magnetic flux enclosed between adjacent contours is 0.032 rads (h/128e). (a)–(f) reprinted with permission from Taylor and Francis.

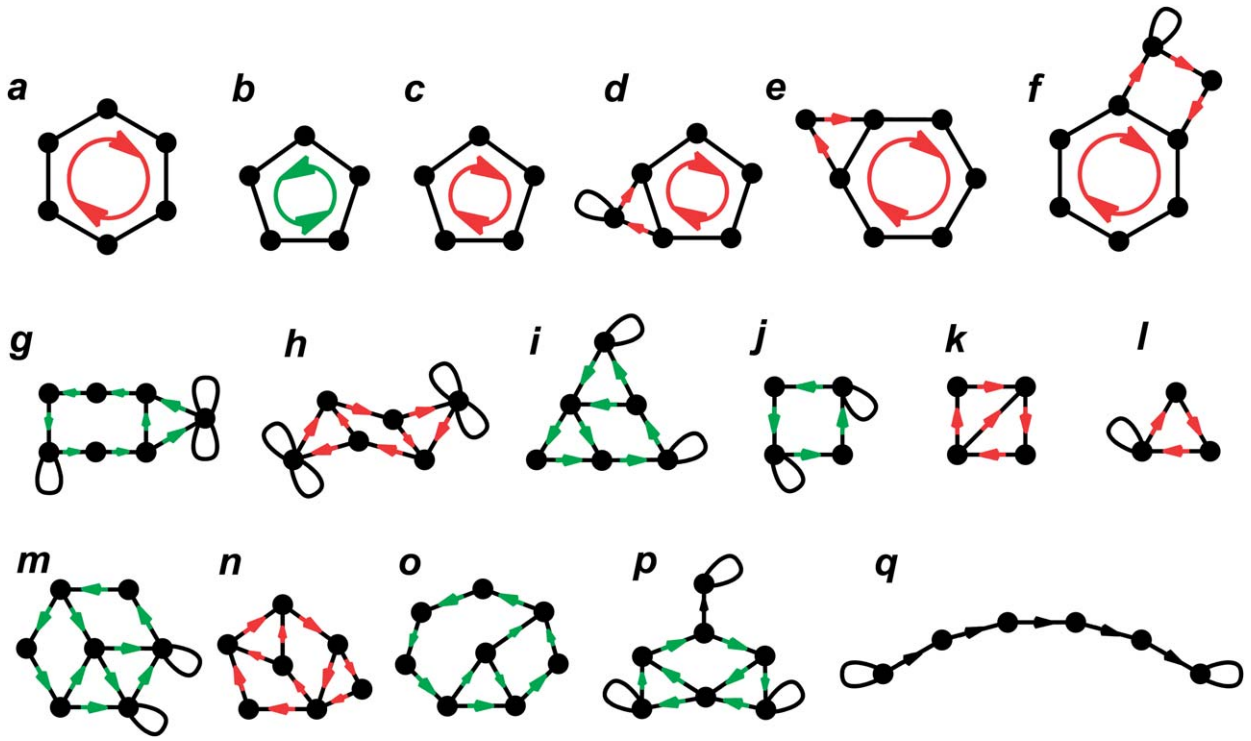

Fig. 9 Line-bond formalism for describing FC states and dipolar couplings within MNP clusters, according to the EH analysis above; arrowheads indicate net direction of magnetic flux between MNPs.

analysis prior to analysis at zero field, and is presumed to have no effect on the statistical (racemic) distribution of CW and CCW polarizations.[20] However, the initial H_z exposure has an important setting function, and dictates the responses of FC states to subsequent magnetic field gradients.

For field-induced switching, coaxial magnetic "pulses" can be applied in alternating directions by modulating the current in the TEM objective lens, followed by a recording of FC polarizations at zero field in between pulses.[22] The retention of polarization by the MNP rings is surprisingly robust: the FC states are not switched after applying $+H_z$ fields as high as 2 Tesla, although minor perturbations in magnetic flux can be observed.[31] However, roughly 90% of the bracelet-like MNP rings experience a switch in FC polarization after exposure to magnetic pulses in the opposite ($-H_z$) direction.[34] The threshold for the H_z-induced FC switching is determined by the collective magnetization (coercivity) of the MNP ring, which depends more on magnetocrystalline anisotropy and the dipolar coupling between NPs than on ring size. For example, the FC polarizations in rings assembled from polycrystalline Co NPs can be reversed by H_z pulses between -0.16 and -0.25 T (Fig. 10), whereas those assembled from single-crystal Co NPs require switching fields between -0.25 and -0.40 T.[22]

Once switched, the FC polarization in MNP rings is unaffected by additional magnetic pulses in the $-H_z$ direction. On the other hand, multiple FC reversals can be achieved by applying pulses in alternating $+H_z$ and $-H_z$ directions.[22] Most remarkably, the scrambling of FC states is not observed, even though the in-plane magnetization is orthogonal to the coaxial magnetic field.

The H_z-induced switching mechanism appears to be quite general, much like the FC states themselves. For example, the FC polarizations of an elliptical MNP ring ($N = 7$), a close-packed square ($N = 4$), and a hexagonal close-packed cluster ($N = 7$) can all be switched by applying a magnetic field in the $-H_z$ direction (Fig. 11). However, the restoration of FC states in these clusters is not as consistent as that observed for the more symmetric MNP rings: "dark patches" in some regions of the phase contour maps can be seen, indicative of residual out-of-plane

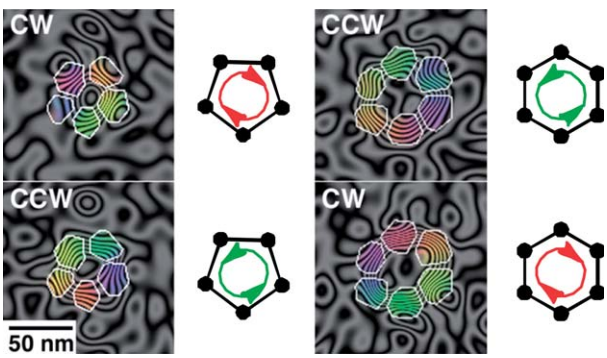

Fig. 10 EH analysis of MNP rings assembled from polycrystalline Co NPs, after exposure to a coaxial (H_z) magnetic pulse.[22] Magnetic induction maps were acquired at zero field. *Top row*, initial FC states with prior exposure to a +2 T field; *bottom row*, FC states after exposure to a -0.25 T field. Magnetic flux enclosed between adjacent contours is 0.065 rads ($h/64e$). Reprinted with permission from Wiley-VCH Verlag GmbH.

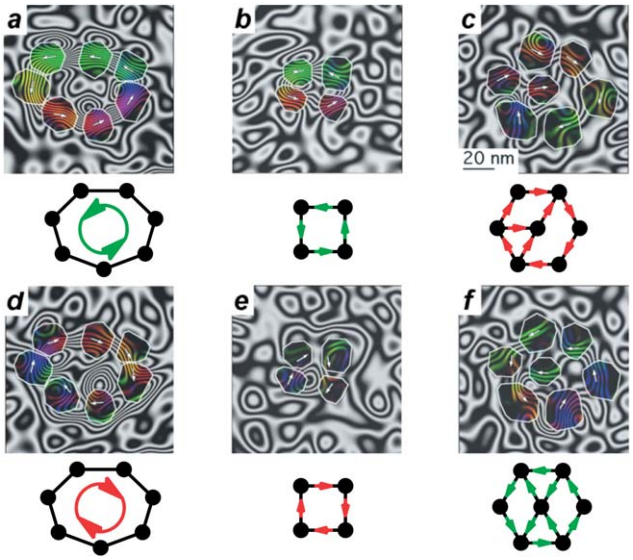

Fig. 11 FC polarizations and magnetic induction maps of other MNP clusters: elliptical 7-membered ring (a and d); close-packed square cluster (b and e); hexagonal close-packed cluster (c and f). Magnetic induction maps were acquired at zero field. (a–c) Initial FC states with prior exposure to a +2 T field; (d–f) FC states after exposure to a −0.16 T field. Magnetic flux enclosed between adjacent contours is 0.065 rads (h/64e).

magnetization.[35] Nevertheless, the FC state is the dominant form of collective magnetization at zero field.

The fidelity in H_z-induced FC switching indicates a strong correlation with prior coaxial magnetizations, *i.e.*, a memory effect. Additional insights into the switching mechanism can be gleaned from magnetodynamic calculations of the FC reversals in a MNP ring after exposure to alternating magnetic pulses ($H_z = \pm 2$ T).[22] These simulations not only reproduce the FC

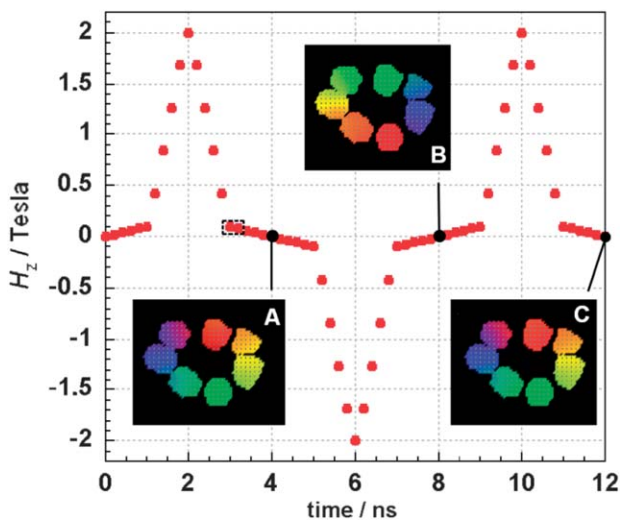

Fig. 12 Magnetodynamic simulations of FC switching in a Co NP ring (*cf.* Fig. 11a), following exposure to alternating H_z pulses.[22] (A) Initial FC state (CW) at zero bias after a +2 T pulse; (B) FC reversal to CCW after a −2 T pulse; (C) second FC reversal to CW after another +2 T pulse. Reprinted with permission from Wiley-VCH Verlag GmbH.

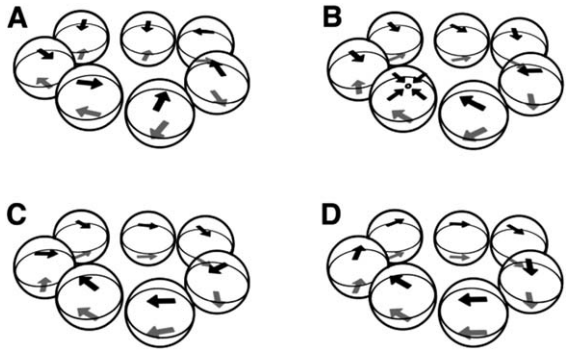

Fig. 13 Transitions in the in-plane magnetization of a MNP ring, derived from magnetodynamic simulations at H_z values between +0.1 and +0.08 Oe (dashed box in Fig. 12).[22] (A) Antiparallel alignment of subdomains in individual MNPs, forming the intermediate double-vortex state; (B) destabilization of the collective state by localized singularities; (C) restoration of single domains within individual MNPs; (D) reformation of a coherent FC state. Reprinted with permission from Wiley-VCH Verlag GmbH.

polarization switching observed by EH analysis at zero field (Fig. 12), but also describe transitions in magnetic induction within MNP rings at variable H_z. For example, the simulations support the existence of a novel intermediate state at low H_z from +0.10 to +0.08 T, just prior to FC reformation. The in-plane magnetization within this "double vortex" state can be described as antisymmetric FC bidomains, with the upper and lower halves of the MNP ring polarized in opposite directions (Fig. 13A). The double-vortex state is metastable and annihilated when H_z drops below +0.08 T (Fig. 13B and C), with subsequent restoration of the FC state (Fig. 13D).

The H_z-induced FC switching mechanism has not been previously described in mesoscale magnetism, and may possibly represent a unique phenomenon for MNP rings. In this regard, it is interesting to note that magnetodynamic simulations of a *continuous* magnetic nanoring do not produce the desired FC reversals upon exposure to alternating H_z pulses, but breaking

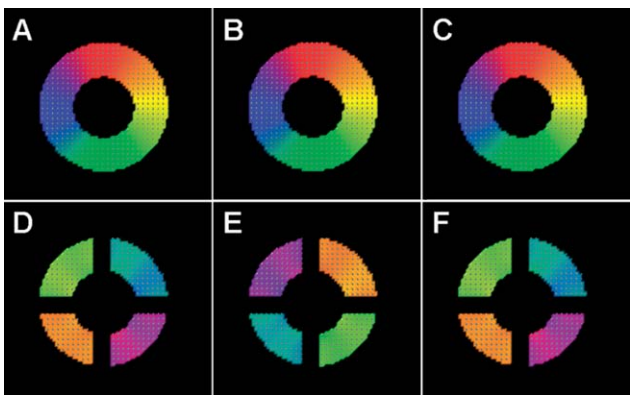

Fig. 14 Magnetodynamic simulations of FC switching in a Co nanoring (o.d. 88 nm; i.d. 22 nm) and a quartered nanoring, following exposure to alternating H_z pulses. (A and D) Initial FC states at zero field after a +2 T pulse; (B and E) FC states after a −2 T pulse; (C and F) FC states after a second +2 T pulse.

the ring into quartered sections restores the FC switching mechanism (Fig. 14).

The physical basis for the correlated FC switching in MNP rings by alternating H_z fields has not yet been fully established, but our simulations indicate a residual moment in the z direction at zero field (*ca.* 10^{-4} G), aligned in the direction of the prior H_z exposure. It will be interesting to determine whether this residual magnetization is sufficient to support the observed memory effect.

Conclusions and outlook

The dipole-directed assembly of thermoremanent MNPs into rings has been discussed for decades, but reproducible conditions for this have only been established in the last ten years. Ring self-assembly can be driven enthalpically by dipolar interactions, and also depends on the MNP concentration and dispersion (entropic factors) and their careful deposition onto surfaces for structural analysis. Macrocyclic surfactants such as calixarene **1** can provide excellent control over the self-assembly and deposition of Co NP rings. It is worth noting that such multivalent surfactants also provide opportunities to direct nucleation and growth processes during Co NP synthesis.[36]

Once formed, MNP rings can be analyzed by electron holography for characterization of their collective magnetic states at zero field. Our studies show that bistable FC states are the dominant form of magnetization at room temperature in bracelet-like MNP rings and also in close-packed clusters, despite large variations in geometry or particle arrangement. The FC polarizations in MNP rings can be reversibly switched by magnetic fields, with appealing potential for applications in NVRAM and magnetoelectronics. We have also identified a novel FC switching mechanism based on H_z-induced magnetic fields, with a strong correlation between FC reversals and the history of prior coaxial magnetizations. Magnetodynamic simulations suggest that the H_z-induced FC switching mechanism may be unique to MNP rings.

The stability of binary FC states in MNP rings (and magnetic nanorings in general) at room temperature suggests many exciting directions for their use in nanoscale switches and memory devices. Nanosized memory cores based on current-induced FC switching may be designed by integrating magnetic nanorings with electrically conductive materials, with potential for further development into 3D nanoscale architectures. Multiple self-assembly approaches may be considered here: For example, MNPs can first be assembled around Au nanoposts by electrophoresis,[37] then annealed into rings defined by dipolar interactions. Another possibility is to deposit MNP rings onto metal substrates with ordered, submicron-sized wells, such as the dimpled surfaces produced by the controlled anodic oxidation of aluminium.[38]

The intriguing effects of size and structure on FC switching offer uncharted opportunities for fundamental studies in nanoscale magnetism and the collective properties of magnetic nanomaterials. While bracelet-sized MNP rings largely support bistable FC states, we have observed that larger, macrocyclic MNP rings can support several other remanent modes at zero field.[39] Continued research in this area is likely to yield a wealth of interesting and surprising findings, with unexpected consequences for future developments in magnetic materials.

Notes and references

1 J.-G. Zhu, Y. Zheng and G. A. Prinz, *J. Appl. Phys.*, 2000, **87**, 6668–6673.
2 C.-L. Chien, F. Q. Zhu and J.-G. Zhu, *Phys. Today*, 2007, (June), 40–45.
3 J. Rothman, M. Kläui, L. Lopez-Diaz, C. A. F. Vaz, A. Bleloch, J. A. C. Bland, Z. Cui and R. Speaks, *Phys. Rev. Lett.*, 2001, **86**, 1098–1101.
4 S. P. Li, D. Peyrade, M. Natali, A. Lebib, Y. Chen, U. Ebels, L. D. Buda and K. Ounadjela, *Phys. Rev. Lett.*, 2001, **86**, 1102–1105.
5 A. P. Griefer, *IEEE Trans. Magn.*, 1969, **5**, 774–811.
6 L. A. Russell, R. M. Whalen and H. O. Leilich, *IEEE Trans. Magn.*, 1968, **4**, 134–145.
7 I. Tudosa, C. Stamm, A. B. Kashuba, F. King, H. C. Slegmann, J. Stohr, G. Ju, B. Lu and D. Weller, *Nature*, 2004, **428**, 831–833.
8 D. Weller and A. Moser, *IEEE Trans. Magn.*, 1999, **35**, 4423–4439; D. Weller and M. Doerner, *Annu. Rev. Mater. Sci.*, 2000, **30**, 611–644.
9 L. J. Heyderman, C. David, M. Kläui, C. A. F. Vaz, J. Rothman and J. A. C. Bland, *J. Appl. Phys.*, 2003, **93**, 10011–10013.
10 J. R. Thomas, *J. Appl. Phys.*, 1966, **37**, 2914–2915.
11 H. Niu, Q. Chen, H. Zhu, Y. Lin and X. Zhang, *J. Mater. Chem.*, 2003, **13**, 1803–1805; G. Cheng, D. Romero, G. T. Fraser and A. R. Hight Walker, *Langmuir*, 2005, **21**, 12055–12059; J. Gao, B. Zhang, X. Zhang and B. Xu, *Angew. Chem., Int. Ed.*, 2006, **45**, 1220–1223; P. Y. Keng, I. Shim, B. D. Korth, J. F. Douglas and J. Pyun, *ACS Nano*, 2007, **1**, 279–292.
12 C. P. Bean and J. D. Livingston, *J. Appl. Phys.*, 1959, **30**, S120–S129.
13 P. Jund, S. G. Kim, D. Tománek and J. Hetherington, *Phys. Rev. Lett.*, 1995, **74**, 3049–3052; W. Wen, F. Kun, K. F. Pal, D. W. Zheng and K. N. Tu, *Phys. Rev. E: Stat. Phys., Plasmas, Fluids, Relat. Interdiscip. Top.*, 1999, **59**, R4758–R4761; J. M. Tavares, J. J. Weis and M. M. Telo da Gama, *Phys. Rev. E: Stat., Nonlinear, Soft Matter Phys.*, 2002, **65**, 061201.
14 A. Wei, B. Kim, S. V. Pusztay, S. L. Tripp and R. Balasubramanian, *J. Inclusion Phenom. Macrocyclic Chem.*, 2001, **41**, 83–86.
15 S. L. Tripp, S. V. Pusztay, A. E. Ribbe and A. Wei, *J. Am. Chem. Soc.*, 2002, **124**, 7914–7915.
16 A. P. Philipse and D. Maas, *Langmuir*, 2002, **18**, 9977–9984; H. Lee, A. M. Purdon, V. Chu and R. M. Westervelt, *Nano Lett.*, 2004, **4**, 995–998.
17 A. Sugawara, K.-I. Fukunaga, M. R. Scheinfein, H. Kobayashi, H. Kitagawa and A. Tonomura, *Appl. Phys. Lett.*, 2007, **91**, 262513.
18 M.-J. Hu, Y. Lu, S. Zhang, S.-R. Guo, B. Lin, M. Zhang and S.-H. Yu, *J. Am. Chem. Soc.*, 2008, **130**, 11606–11607.
19 Y. Xiong, J. Ye, X. Gu and Q.-W. Chen, *J. Phys. Chem. C*, 2007, **111**, 6998–7003; Y. Zhai, J. Zhai and S. Dong, *Chem. Commun.*, 2010, **46**, 1500–1502; H. Wang, Q.-W. Chen, Y.-B. Sun, M.-S. Wang, L.-X. Sun and W.-S. Yan, *Langmuir*, 2010, **26**, 5957–5962.
20 S. L. Tripp, R. E. Dunin-Borkowski and A. Wei, *Angew. Chem., Int. Ed.*, 2003, **42**, 5591–5593.
21 R. E. Dunin-Borkowski, T. Kasama, A. Wei, S. L. Tripp, M. J. Hytch, E. Snoeck, R. J. Harrison and A. Putnis, *Microsc. Res. Tech.*, 2004, **64**, 390–402; J. M. Thomas, E. T. Simpson, T. Kasama and R. E. Dunin-Borkowski, *Acc. Chem. Res.*, 2008, **41**, 665–674.
22 T. Kasama, R. E. Dunin-Borkowski, M. R. Scheinfein, S. L. Tripp, J. Liu and A. Wei, *Adv. Mater.*, 2008, **20**, 4248–4252.
23 A. Wei, *Chem. Commun.*, 2006, 1581–1591.
24 Z. Chen, J. Liu and A. Wei, unpublished results.
25 K. V. P. M. Shafi, I. Felner, Y. Mastai and A. Gedanken, *J. Phys. Chem. B*, 1999, **103**, 3358–3360; W. L. Zhou, J. B. He, J. Y. Fang, T. A. Huynh, T. J. Kennedy, K. L. Stokes and C. J. O'Connor, *J. Appl. Phys.*, 2003, **93**, 7340–7342; L. V. Govor, G. H. Bauer, G. Reiter, E. Shevchenko, H. Weller and J. Parisi, *Langmuir*, 2003, **19**, 9573–9576; H. Gu, B. Xu, J. Rao, R. K. Zheng, X. X. Zhang, K. K. Fung and C. Y. C. Wong, *J. Appl. Phys.*, 2003, **93**, 7589–7591; Z. Liu and R. Levicky, *Nanotechnology*, 2004, **15**, 1483–1488.
26 P. C. Ohara, D. V. Leff, J. R. Heath and W. M. Gelbart, *Phys. Rev. Lett.*, 1995, **75**, 3466–3469; P. C. Ohara and W. M. Gelbart,

Langmuir, 1998, **14**, 3418–3424; T. Vossmeyer, S.-W. Chung, W. M. Gelbart and J. R. Heath, *Adv. Mater.*, 1998, **10**, 351–353.
27 M. Maillard, L. Motte and M. P. Pileni, *Adv. Mater.*, 2000, **13**, 200–204.
28 J. Gómez-Segura, O. Kazakova, J. Davies, P. Josephs-Franks, J. Veciana and D. Ruiz-Molina, *Chem. Commun.*, 2005, 5615–5617; B. P. Khanal and E. R. Zubarev, *Angew. Chem., Int. Ed.*, 2007, **46**, 2195–2198.
29 R. D. Deegan, O. Bakajin, T. F. Dupont, G. Huber, S. R. Nagel and T. A. Witten, *Nature*, 1997, **389**, 827–829.
30 R. F. Egerton, *Electron Energy Loss Spectroscopy in the Electron Microscope*, Plenum Press, New York, 1996.
31 A. Wei, S. L. Tripp, J. Liu, T. Kasama and R. E. Dunin-Borkowski, *Supramol. Chem.*, 2009, **21**, 189–195.
32 M. Kläui, J. Rothman, L. Lopez-Diaz, C. A. F. Vaz and J. A. C. Bland, *Appl. Phys. Lett.*, 2001, **78**, 3268–3270; U. Welp, V. K. Vlasko-Vlasov, J. M. Hiller, N. J. Zaluzec, V. Metlushko and B. Ilic, *Phys. Rev. B: Condens. Matter Mater. Phys.*, 2003, **68**, 054408; F. Q. Zhu, G. W. Chern, O. Tchernyshyov, X. Zhu, J.-G. Zhu and C.-L. Chien, *Phys. Rev. Lett.*, 2006, **96**, 027205.
33 K. Bussmann, G. A. Prinz, R. Bass and J.-G. Zhu, *Appl. Phys. Lett.*, 2001, **78**, 2029–2030.
34 Negative Hz pulses were effectively obtained by turning the specimen over by 180 degrees within the TEM: T. Kasama, R. E. Dunin-Borkowski, M. R. Scheinfein, S. L. Tripp, J. Liu and A. Wei, *C-MRS Int. Symp. Proc.*, 2007, **1026E**, C18.03.
35 In some images, artifacts during image processing can also contribute to the loss of phase contrast.
36 J. Liu and A. Wei, *Chem. Commun.*, 2009, 4254–4256.
37 Q. K. Ong, PhD thesis, Purdue University, 2010.
38 H. Masuda and K. Fukuda, *Science*, 1995, **268**, 1466–1468.
39 T. Kasama, J. Liu, Z. Chen, M. Bellegia, R. E. Dunin-Borkowski and A. Wei, unpublished results.